MODELING OF IRON OXIDATION IN A PASSIVE TREATMENT SYSTEM[1]

by

George R. Watzlaf[2], Karl T. Schroeder and Candace L. Kairies

Abstract. Iron oxidation rates were modeled in a passive system using pH, temperature, dissolved oxygen and iron concentrations. The system consists of a 224 meter ditch receiving the effluent from an anoxic limestone drain (ALD), which treats drainage from a reclaimed surface coal mine in Clarion County, Pennsylvania. The ditch was divided into ten sections. Depth and width were measured for each section. Three water samples (raw, unfiltered and acidified, filtered and acidified) were collected at the beginning and end of each section. Water analyses included field-measured pH, dissolved oxygen, and temperature, and laboratory-measured net acidity and major and trace elemental concentrations (including Fe^{2+}, Fe_{TOT}, Ca, Al, Na, Mn, SO_4^{2-}, K, As, Ba, Be, Cd, Co, Cr, Cu, Ni, Pb, Sb, Se and Zn). Field pH, dissolved oxygen and temperature varied between 5.89 - 6.37 s.u., 0.52 - 7.75 mg/L, and 12.1 - 22.0°C, respectively. The average flow rate for the system was 92.8 L/min. Iron concentration decreased to approximately 70% of the original level by the end of the ditch. A kinetic model for loss of ferrous iron from solution was compared to the traditional sizing criteria for iron removal of 10 - 20 $gd^{-1}m^{-2}$. Because of the geometry of the ditch, a plug flow model was used. The majority of the sections had removal rates near the 20 $gd^{-1}m^{-2}$ traditional value, and modeling provided insight as to why certain sections performed better than others. All significant changes occurred soon after aeration, indicating that net alkaline water should be aerated immediately in order to optimize iron removal.

Additional Key Words: iron oxidation kinetics, iron removal rates, mine drainage.

Introduction

Many passive systems have successfully treated mine drainage over the past decade (Watzlaf et al. 2000). Successful treatment is defined as pH > 6.0, total iron concentration < 3.0 mg/L, and aluminum concentration < 1.0 mg/L. Successful sites are usually those that treat either naturally occurring net alkaline water or water made net alkaline by the use of anoxic limestone drains. Net alkaline drainage is typically characterized by a pH between 6.0 - 6.5, total iron < 150 mg/L (>99% of which in the ferrous form), and dissolved aluminum < 1.0 mg/L. At many of these successful sites, flow rates are less than 100 L/min; however, successful treatment is observed at some sites with much higher flows (~ 300 - 1000 L/min). Ponds, wetlands, ditches and waterfalls are used to passively aerate the water, oxidize the ferrous iron (equation 1), precipitate the ferric hydroxide (equation 2), and settle the precipitates.

$$Fe^{3+} + 3H_2O \rightarrow Fe(OH)_3 + 3H^+ \qquad (1)$$

$$Fe^{2+} + 1/4O_2 + H^+ \rightarrow Fe^{3+} + 1/2H_2O \qquad (2)$$

Empirically-derived sizing criteria have been developed based on surface area (Hedin et al. 1994). These criteria have been used to size dozens of systems worldwide. Hedin et al. (1994) studied several ponds,

[1]Paper presented at the 2001 National Meeting of the American Society for Surface Mining and Reclamation. Albuquerque, New Mexico, June 3-7, 2001. Pub. by ASSMR 3134 Montavesta Rd., Lexington, KY 40502.

[2]George R. Watzlaf, Environmental Engineer, Karl T. Schroeder, Chemist, Candace L. Kairies, Environmental Scientist, .National Energy Technology Laboratory, U. S. Department of Energy, Pittsburgh, PA 15236.

Proceedings America Society of Mining and Reclamation, 2001 pp 626-638
DOI: 10.21000/JASMR01010626

wetlands and ditches and found that dilution-adjusted iron removal rates in alkaline mine water where load was not limited (i.e., iron concentration did not go to "zero") averaged 23 $gd^{-1}m^{-2}$ and ranged from 6 to 43 $gd^{-1}m^{-2}$. The lower removal rates were attributed to possible short-circuiting and poor aeration, while the higher removal rates were attributed to extremely effective aeration. Their recommended sizing criteria for iron removal was 10 - 20 $gd^{-1}m^{-2}$. The lower removal rate (10 $gd^{-1}m^{-2}$) recognized the need for non-abandoned sites to meet regulatory guidelines (Fe < 3.0 mg/L), as well as the slower removal rates at low iron concentrations. These removal rates have been found to be fairly consistent with other studies (Stark et al. 1990, Brodie 1991). While these criteria are extremely useful "rules of thumb" and seem to work well for the typical passive systems used to treat mine drainage, it should be possible to model iron removal rates using the variables that affect iron oxidation, precipitation and settling. Many of the higher flows of net alkaline mine drainage have yet to be treated because of the uncertainties of iron removal rates and the large areas required by applying these conservative criteria. Successful models would provide better quantitative information for the appropriate sizing of new construction and could provide the mechanistic insight needed for the development of innovative technologies for the future.

This study is limited to modeling the loss of Fe(II) from solution. The modeling is based on the abiotic rate and activation energy equations for iron oxidation. However, the fate of the ferrous iron was not determined and other processes, such as adsorption, cannot be ruled out.

Background

Iron removal is comprised of the oxidation of ferrous iron (equation 1), precipitation of ferric hydroxide (equation 2), and settling of the solids. The major parameters affecting the oxidation of ferrous iron are Fe(II) concentration, pH, dissolved oxygen and temperature. At lower pH values (< 5), iron oxidizing bacteria can significantly accelerate oxidation rates, which would be extremely slow abiotically (Singer and Stumm 1970). At pH values > 5.5 (conditions at the modeled site), the abiotic oxidation rate is much faster than the biotic rate and can be expressed as:

$$\frac{d[Fe(II)]}{dt} = -k \frac{[Fe(II)][O_{2(aq)}]}{[H^+]^2} \quad (3)$$

or alternatively as:

$$\frac{-d\,[Fe(II)]}{dt} = k\,[Fe(II)][OH^-]^2 P_{O2} \quad (4)$$

Stumm and Lee (1961) and Stumm and Morgan (1981), respectively. As can be seen in equation 3, the oxidation of ferrous iron is first order with respect to the concentrations of Fe(II) and dissolved oxygen and inversely proportional to the square of the hydrogen ion concentration. Therefore, a doubling of Fe(II) or dissolved oxygen concentration doubles the reaction rate; however, a one unit increase in pH increases the reaction rate by a factor of 100. Stumm and Morgan (1981) report that for a given pH, the rate of reaction increases about 10-fold for a temperature increase of 15°C. Kirby and Elder Brady (1998) list several other factors reported to affect Fe(II) oxidation rate in natural waters: Cu(II), Co(II), anions which form complexes with Fe(III), organic acids, Na^+, presence of ferric hydroxide solids, ionic strength, sulfate, light intensity, colloidal silica and aluminum oxide, and bentonite clay.

Kirby et al. (1999) modeled Fe(II) oxidation in 17 ponds at six passive treatment facilities based on published biotic and abiotic laboratory rate laws. Using Fe(II) concentration, pH, temperature, *Thiobacillus ferrooxidans* population, dissolved oxygen concentration, flow rate, and pond volume; reasonably accurate predictions of iron oxidation could be made. Between pH 2.8 - 5, Fe(II) oxidation rates were negatively correlated with pH and catalyzed by *T. ferrooxidans*. Between pH 5 - 6.4, oxidation rates were primarily abiotic and positively correlated with pH. Above pH 6.4, they found no correlation with pH.

The hydrolysis of ferric iron is not usually rate-limiting at the pH values found in net alkaline mine water (typically between 6.0 and 7.0). Once ferrous iron is oxidized, the hydrolysis of ferric iron occurs extremely rapidly. Singer and Stumm (1970) reported the hydrolysis is fourth order with respect to pH.

The limited goal of this study was to quantitatively model the ferrous iron oxidation at a functioning remediation site. The site described here was chosen because it was thought that its regular geometry would minimize the number of flow paths and provide near plug-flow conditions. Therefore, this study differs in approach to others that treat ponds and wetlands as continuously-stirred tank reactors (Kirby et al. 1999).

Site Description

The system treats drainage from a reclaimed surface coal mine in Clarion County, Pennsylvania. Effluent from an ALD flows through a 224 meter ditch, which averages 3 meters in width (Figure 1). The upper section of the ditch (section AD, see Figure 1) is virtually flat with a measured slope of 0.1%. Section DE is steeply sloped (23%). Section EI is gently sloped (0.5%) and contains three areas of cattails. Section IJ is another steeply sloped section (16%) that contains a weir at point J. Complete water quality analysis at the beginning (point A) and end (point K) of the ditch is presented in Table 1.

Methods

As shown in Figure 1, the ditch was divided into ten sections, A through K. Several width and depth measurements were taken for each section. Average values of these measurements were used to calculate surface area and volume for each section. Three 150-mL samples were collected at the beginning and end of each section: an unfiltered unacidified sample (raw), an unfiltered acidified sample, and a filtered acidified sample. The filtered sample was filtered through a 0.2μm syringe filter prior to acidification. Samples were acidified by adding 2.0 mL of concentrated HCl, which lowered the pH to below 1.0. All pH measurements were made using the Orion 250A portable meter with standard pH electrodes. The pH meter was calibrated with standard buffer solutions (pH 4 and pH 7, which bracketed all measured field pH values) prior to measurement at the site. Alkalinity was measured in the field using the Hach Digital Titration method. Dissolved oxygen (DO) and temperature were measured in the field using the YSI Model 55 Handheld Dissolved Oxygen and Temperature System. Flow rates were measured at the effluent of the ALD (sample point A) and at a weir near the end of the ditch (sample point J) using timed volumetric measurements (bucket and stopwatch method).

Samples were transported to the analytical laboratory and analyzed using standard methods. Acidity was determined by adding H_2O_2 to the sample, and then heating and titrating the solution to pH 8.2 with NaOH (American Public Health Association, 1998). Major and trace elemental concentrations (including Fe, Ca, Al, Na, Mg, Mn, K, As, Ba, Be, Cd, Co, Cr, Cu, Ni, Pb, Sb, Se and Zn) in the acidified samples were determined using inductively coupled argon plasma - atomic emission spectroscopy (ICP-AES). Ferrous iron concentrations were determined by titration with $K_2Cr_2O_7$ (Fales and Kenny, 1940). Sulfate concentrations were determined by ICP-AES (as total sulfur) on water samples that had been acidified and boiled to remove any hydrogen sulfide.

The volume of water in each section of the ditch was determined using the measurements made in the field. Measured flow at the weir was 9% lower than measured flow at the ALD effluent. To estimate flow for each section, it was assumed that the apparent losses were uniform throughout the ditch. Prorated flows for each sampling point were calculated by dividing the distance (of the sampling point) in the ditch from the ALD by the total length of the ditch, and multiplying this quantity by the difference in the two measured flows. Detention times (t_d) for each section were calculated based on volume and these prorated flows.

Table 1. Influent and effluent water quality.

Parameter	In	Out	Parameter	In	Out
Flow (L/min)[1]	97.2	88.4	Aluminum (mg/L)	0.41	<0.10
Temperature (°C)[1]	12.1	21.2	Calcium (mg/L)	201	201
Dissolved Oxygen (mg/L)[1]	0.23	7.75	Magnesium (mg/L)	118	120
pH (S.U.)[1]	5.89	6.27	Cobalt (mg/L)	0.72	0.74
Alkalinity (mg/L as $CaCO_3$)[1]	149	15	Nickel (mg/L)	0.84	0.88
Iron (mg/L)	216	157	Zinc (mg/L)	1.51	1.33
Net Acidity (mg/L as $CaCO_3$)	279	303	Barium (mg/L)	0.02	0.03
Sulfate (mg/L)	1200	1230	Potassium (mg/L)	6.08	6.70
Manganese (mg/L)	40.8	42.2	Sodium (mg/L)	5.44	6.66

Elements below detection limits include: As, Be, Cd, Cr, Cu, Pb, Sb, Se.
[1]Parameters measured in the field.

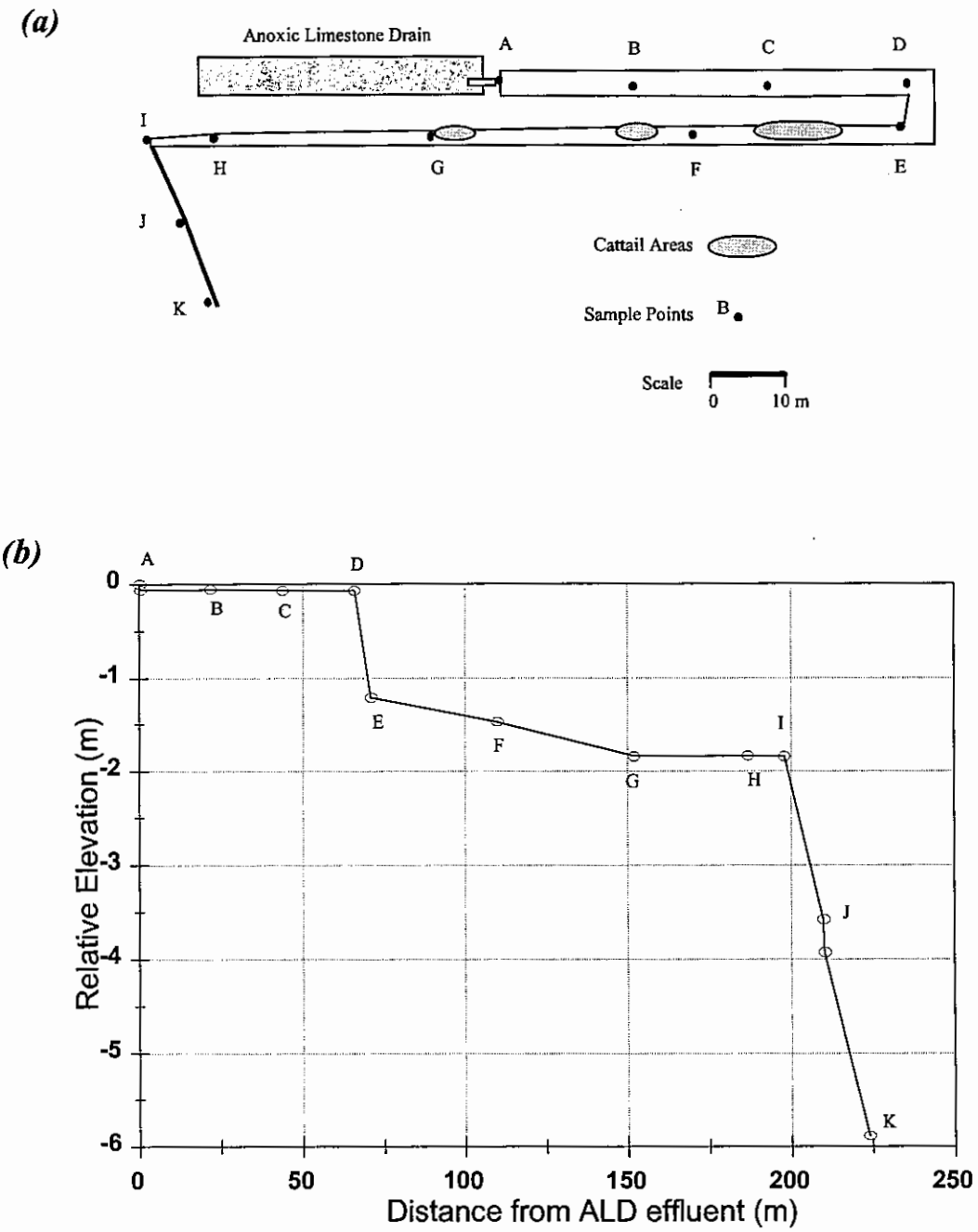

Figure 1. (a) Plan view of passive treatment site and (b) elevation of water surface as a function of distance from ALD effluent.

Results and Discussion

Water Quality Trends

Table 1 presents the water quality in and out of the 224 m ditch. Most of these parameters remained fairly constant from sample point to sample point. Only four measured parameters underwent significant changes as the water flowed through the ditch: dissolved oxygen, pH, temperature, and iron (total, total dissolved, and ferrous). Figure 2 graphs these parameters as a function of distance from the ALD effluent pipe.

The ditch can be separated into four main parts: the upper ditch (section AD), the steeply-sloped bend (section DE), the lower ditch (section EI), and the final steeper section that contained a weir (section IK) (see Figure 1). The upper ditch (AD) can be characterized as fairly deep (~0.5 m), wide (3 m), and flat (0.1% slope), with very slow moving water (average velocity = 0.087 m/min). The steeply-sloped (23% slope) bend (DE) contained shallow water (~0-6 cm), was spread out (4.5 m wide) and flowed turbulently over and around numerous rocks (rip rap). Theoretical detention time in this section (which included a part of the upper and lower ditches) was 37 min. The lower ditch (EI) was moderately sloped (0.5%), ranged in width from 1-4 m, was fairly shallow (1-4 cm), and contained some small riffles and three areas of cattails. The theoretical detention time of this lower ditch was 82 min. The final part was steeply sloped (16%), fairly shallow (1- 6 cm) and narrow (38 cm) with turbulent flow. A weir was positioned about the midpoint of this section (point J). The theoretical detention time of this part was 4.2 min.

As the water flowed out of the ALD, DO was near zero (0.23 mg/L). The water dropped only 1 - 2 cm from the bottom of the pipe to the water level in the upper ditch and flowed in a narrow channel for a distance of about 1 m before it spread out into the full width and depth of the upper ditch. At the end of this narrow channel (1 m from the ALD effluent pipe), DO was only 0.52 mg/L. As the water flowed through the remainder of the upper part of the ditch (section AD), DO slowly increased to 4.46, after a theoretical detention time of about 760 min. Within the upper ditch, pH increased less than 0.1 unit, from 5.89 to 5.97. Because there was very little agitation, only small amounts of carbon dioxide was presumably able to degas, which kept the pH from increasing significantly. Temperature increased from 12.1 to 17.7 ° C. Total dissolved iron decreased only 2.2 mg/L, from 216.2 to 214.4 mg/L.

Very significant changes occurred in the steeply-sloped bend (DE). Dissolved oxygen increased from 4.46 to 7.04 mg/L. At the measured temperatures (17.2 and 17.7 ° C), this amounted to a change from 46% to 74% saturation. This was very effective aeration considering that this 2.58 mg/L increase in DO occurred in a matter of minutes, compared to the change in the upper ditch of 4.23 mg/L, which took over 12 hours. Presumably, this agitation also caused a significant degassing of carbon dioxide as evidenced by a jump in pH from 5.97 to 6.34. With the addition of DO and increase in pH, total dissolved iron showed a decrease of 9.7 mg/L (214.4 to 204.7 mg/L).

In the lower ditch, DO and pH remained fairly constant, 7.04 to 6.88 mg/L and 6.34 to 6.19 s.u., respectively. Temperature continued to increase (17.7 to 22.0 ° C), reaching air temperature. Because DO and pH remained relatively high, iron continued to be oxidized. Iron concentrations went from 204.7 to 158.7 mg/L.

It took the water only 4.2 min to traverse the final 26 meters of the ditch. In this area, DO increased from 6.88 to 7.75 mg/L and pH increased from 6.19 to 6.27 s.u. Only a minor change in iron was realized, 158.7 to 157.0 mg/L, presumably due to the very short detention time of this section.

The largest changes in pH, DO, and iron, with respect to detention time occurred after point D where the water underwent effective aeration. Prior to point D (the upper ditch), no significant changes in pH or iron were observed. Dissolved oxygen did increase from 0.23 to 4.46 mg/L over the 12-hours detention time.

Iron Removal Rates

Table 2 displays iron removal rates in $gd^{-1}m^{-2}$ for each section of the ditch, as well as for combinations of sections. To calculate these removal rates, total dissolved iron values were used. Turbulent flow in some sections contained a significant amount of suspended iron precipitate. The dissolved iron values indicate what the total iron concentration would be after settling of the solids. Individual removal rates for each section were quite variable. Much of this can be attributed to the very small changes in iron concentration within each section. Iron concentration differences often approached the analytical variability of the analysis. When sections are combined, however, a clearer picture of iron removal is obtained. For the top, quiescent part of the ditch (AD), iron removal rates measured only 0.4 $gd^{-1}m^{-2}$. The iron value at point B was actually higher than point A, presumably due to analytical variation. Calculating iron

(a)

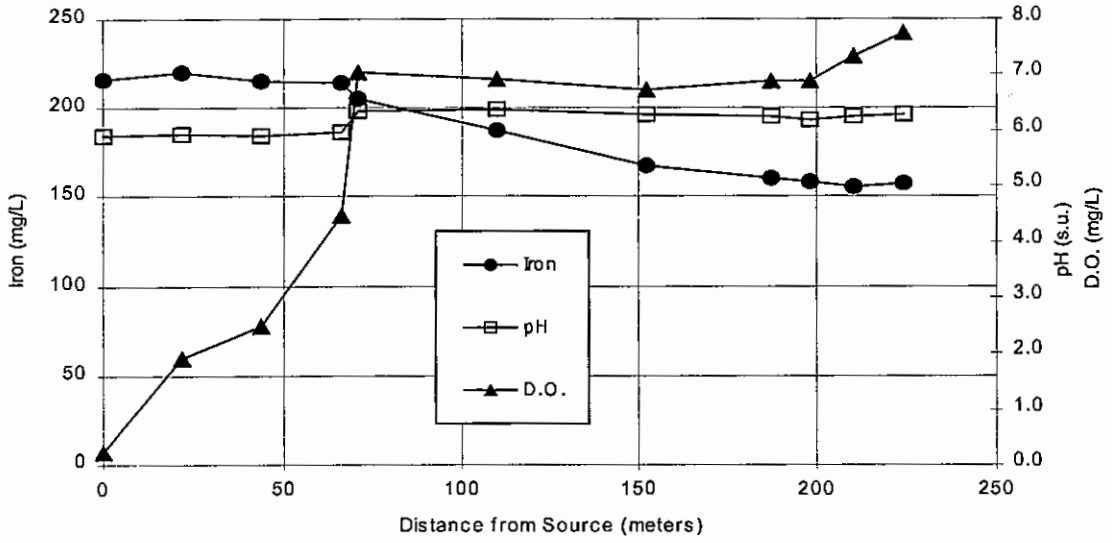

(b)

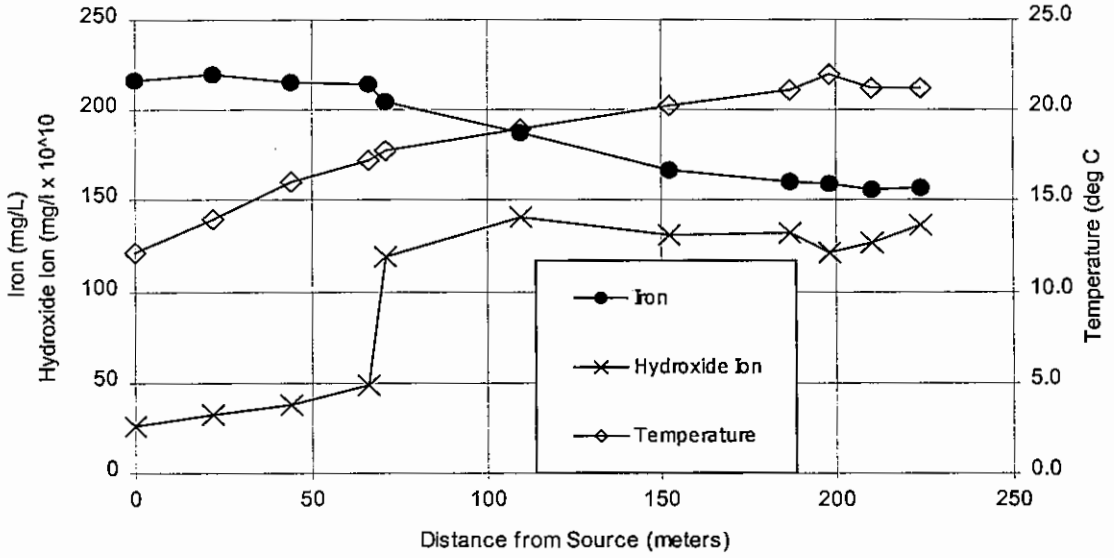

Figure 2. Change in variables known to be important to iron oxidation kinetics as a function of distance of the sampling location from the mine drainage source. (a) iron (left axis) overlay with DO concentration and pH (right axis). (b) iron and hydroxide concentrations (left axis) overlay with temperature (right axis). Note the sharp rise in DO and hydroxide concentration about 70 meters down-stream corresponding to points D and E in Figure 1.

Table 2. Iron concentration, prorated flow, surface area and iron removal rate at selected sections.

Section	Total Dissolved Fe IN (mg/L)	Total Dissolved Fe OUT (mg/L)	Flow (L/min)	Surface Area (m^2)	Removal Rate ($gd^{-1}m^{-2}$)
AB	216.2	219.7	96.8	82.5	-5.9
BC	219.7	215.5	95.9	96.8	6.0
CD	215.5	214.4	95	91.3	1.6
DE	214.4	204.7	94.5	39.3	33.6
EF	204.7	187.7	93.7	117	19.6
FG	187.7	167.0	91.9	101	27.2
GH	167.0	160.5	90.4	70.0	12.1
HI	160.5	158.7	89.6	13.2	17.6
IJ	158.7	155.8	89.1	4.88	76.2
JK	155.8	157.0	88.6	4.98	-30.7
AD	216.2	214.4	95.9	271	0.4
BD	219.7	214.4	95.5	187	3.9
DI	214.4	158.7	91.9	340	21.7
DK	214.4	157.0	90.4	350	21.3
EI	204.7	158.7	91.1	301	20.2
EK	204.7	157.0	90.0	311	19.9
IK	158.7	157.0	88.4	9.86	21.9
AK	216.2	157.0	92.8	621	12.7

Negative removal rates indicate an increase in iron concentration and are presumably due to analytical variation.

removal for BD still only yields a value of 3.9 $gd^{-1}m^{-2}$. However, once the water is aerated (section DE), iron removal rates for combinations of the following sections are very consistent. For the lower part of the ditch (EI), the removal rate is 20.0 $gd^{-1}m^{-2}$. In fact all combinations of sections after the turbulent flow section DE display very similar iron removal rates, DI = 21.7 $gd^{-1}m^{-2}$, DK = 21.3 $gd^{-1}m^{-2}$, EK = 19.9 $gd^{-1}m^{-2}$, and IK = 21.9 $gd^{-1}m^{-2}$. The overall removal rates for the entire ditch (AK) was 12.7 $gd^{-1}m^{-2}$. This overall removal rate and the rates after the point of aeration (D) are consistent with the removal rates reported by Hedin et al. (1994).

Modeling

The iron concentration, DO concentration, pH and temperature all changed as the water flowed through the system. The initial ALD effluent had low DO and pH and high ferrous iron concentration. As the water passed through the system, the DO and pH increased, especially in a particularly turbulent section (section DE in Figure 1), and the ferrous iron level, which was initially 216 mg/l decreased to an effluent level of about 157 mg/l. One objective of the current study was to account for the iron removal quantitatively. The basis for the modeling was the well established rate and temperature dependence formulae. It was found that these formulae were indeed able to model the system but, the numerical values obtained were not in the range expected for fundamental processes.

Three types of measurements were needed for the kinetic analysis: time, temperature, and concentration. All of these variables were different at the various sampling locations (Figure 1). The magnitude of these variables as a function of linear distance from the water source (ALD outlet) are shown in Figure 2. Details of the procedures are given in the Methods section.

The water temperature increased from about 12 °C

at the ALD to about 22 °C at the last sampling location (Figure 2b). Temperature is known to affect the rate in a number of ways. Because the dissociation constant for water, K_w, depends on temperature, this change must be taken into account during the conversion from pH, the measured parameter, to hydroxide ion concentration, the rate dependent variable (Equation 5). In this study, K_w values were obtained by linear interpolation between published values (Stumm and Morgan 1996). For reactions with activation energies, that is, those that are not diffusion controlled, the rate constant increases with increasing temperature, so k would not be constant throughout the system. The attempt to account for this using an activation parameter is described below. The temperature also affects the Henry's law constant used to calculate the molar concentration of oxygen from it's partial pressure. However, in this study, dissolved oxygen concentrations were measured directly.

$$K_w = [H^+]\ [OH^-] \qquad (5)$$

At constant temperature, the rate of ferrous iron oxidation is proportional to the ferrous iron concentration, dissolved oxygen concentration and the square of the hydroxide ion concentration. The integrated form of the rate expression is given in Equation 6. In laboratory experiments, it is usually possible to control the pH and oxygen concentration (partial pressure) to constant values. As mentioned above, this was not possible at the field remediation site. In this study, we made the assumption that these variables were constant over each of the individual intervals between sampling locations (Figure 1). We used the average DO between inlet and outlet and the pH at the outlet as the "constant" concentrations in each segment. In this manner, a value for the rate constant, k, was calculated for each segment.

$$\ln \frac{[Fe^{+2}]}{[Fe^{+2}]_o} = -k\ t\ [O_2]\ [OH^-]^2 \qquad (6)$$

To quantitatively model the iron loss throughout the system, the temperature dependence was taken to be an exponential in the same fashion as an activation energy (Equation 7). To determine the temperature coefficient, the natural log of k was plotted against 1/RT. This provided a slope (E_{act}) and an intercept (ln A). In this fashion, the kinetic model was derived for the system. These initial estimates of the activation parameters are described herein as the "linear regression" estimates.

$$k = A\ e^{\frac{-E_{act}}{RT}} \qquad (7)$$

However, it was found that the ferrous iron concentrations could be modeled more precisely by using an additional error minimization routine. In this effort, the linear regression values obtained above were used in a subsequent analysis as the initial estimates of the true E_{act} and ln A in the Solver routine in Microsoft Excel. The design and use of the Solver has been described by Fylstra et al. 1998. In this case, the sum of the squares of the deviations between the calculated and measured ferrous iron concentrations was minimized while allowing only E_{act} and ln A to vary under the restrictions that both had to be positive. Relaxing these restrictions did not change the final solution. This resulted in a new E_{act} and ln A which were also used to predict the ferrous iron concentrations at the various sampling locations. This does not constitute a second model but rather, a different method for determining the numeric values of the variables in a single model. These estimates are described herein as the "solver" estimates.

The measured ferrous iron values are shown as the solid circles and the values calculated by the above procedures are displayed as lines in Figure 3. In this figure, the detention time, rather than linear distance is used for the x-axis. The agreement between the measured values and those provided by the model are very good, especially when one considers that only two adjustable parameters, E_{act} and ln A, were used. The figure clearly shows the rapid decrease in iron after a long initial period of little reaction. The break-point corresponds to the position of a rip-rap filled channel between the settling ponds and the wetlands. This five-meter-long section (DE) increases the DO from 4.5 to 7.0 mg/L, increases the pH from 5.9 to 6.3, and dramatically accelerates iron oxidation. The figure also shows that during the first 700 minutes little or no iron oxidation occurred in the large settling area preceding the rip-rap channel because of the unfavorable reaction kinetics.

A better appreciation for the difference between the calculated and observed ferrous iron concentrations can be obtained by viewing only the last 100 minutes of detention time. A zoom-in on this region of the graph is shown in Figure 4. The solid lines (thin and thick) show the correspondence between the measured ferrous iron levels (circles) and the predicted levels based on the linear regression and solver estimates of E_{act} and ln A, respectively. Because the regression line is above all but the first point, the constants derived using the linear regression estimate contain a bias causing the model to

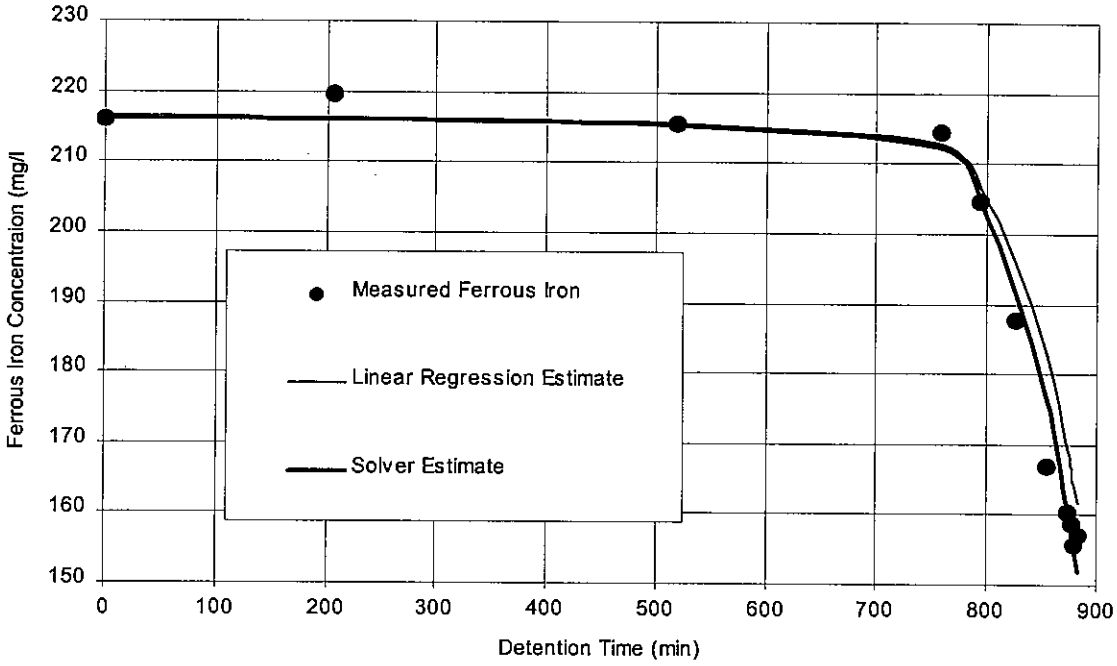

Figure 3. Measured (circles) and predicted (lines) ferrous iron concentrations as a function of total detention time in the remediation system.

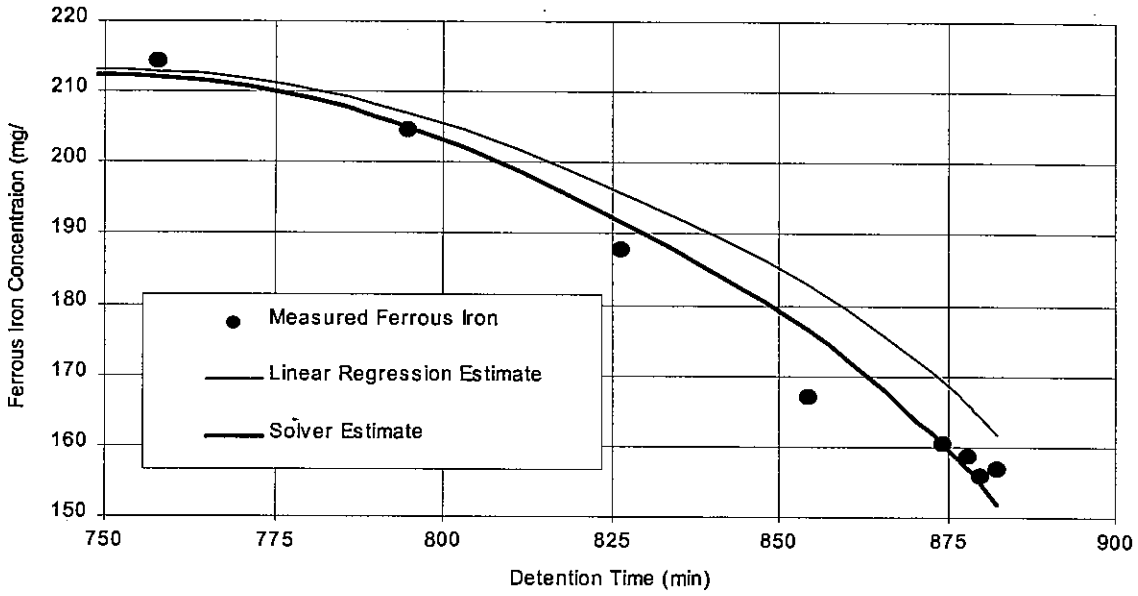

Figure 4. Expanded view of the last eight sampling locations (D through K in Figure 1) where the largest decreases in ferrous iron were observed. Circles are the measured concentrations; lines are from the model.

consistently underestimate the extent of oxidation. The presence of points both above and below the solver line provides some assurance that the bias has been removed in the final error minimization.

It is instructive to compare the numerical values provided by the model to literature values of the activation energy and rate constants. The E_{act} value obtained from the regression and solver estimates and the rate constants at 25°C are compared to the literature in Table 3. It is obvious that there are differences in the fundamental laboratory oxidation reaction reported in the literature and our model using field data. The regression and solver estimates of E_{act} value are equal and much larger than what is reported in the literature. Little temperature dependence is reported after correcting for the effect of temperature on oxygen solubility and K_w (Stumm and Lee 1961). Other factors not considered explicitly in the modeling, such as catalysis by ions and the catalytic and/or adsorptive properties of surfaces, may be playing a role. The small increases in Na and K can account for only 3% of the total Fe loss via ion exchange. Microbial activity is usually not sufficiently high to be a factor at the pH values found here (Stumm and Morgan 1981). Thus, the model should be considered a characterization tool that describes the response of the system to certain variable changes but not necessarily as a mechanistic descriptor of processes at the molecular level. The k-values at 25°C calculated from the model appear to be more reasonable but still higher than the literature values, again indicating the possibility of other removal pathways. However, it should be noted that the highest temperature actually measured at the modeled site was 22°C and that the calculation of $K_{(25°C)}$ involves extrapolation into the region were the rate constant is rapidly changing.

One of the benefits of a model that describes the remediation system is the ability to predict the outcome of system modifications. The result of "what if" scenarios can be used to evaluate the effectiveness of additional treatment options and thus provide rational for, or against, a particular type of construction. However, care must be taken not to generalize the results beyond the system being modeled, especially in those instances, such as appears to be the case here, where more than just the aqueous chemistry is affecting the rate.

We have applied the model, using the solver estimates of E_{act} and ln A, to the evaluation of the effect of changing the values of some of the reaction variables. We investigated one case of worse performance and 4 options for improved performance (Figure 5). The effect of raising or lowering the temperature can be seen by comparing lines 1 and 4 (counting from the top) with the original model depicted in line 2. Temperature is of interest because the large E_{act} predicts large temperature effects and because of the lack of control options for this variable in the field. Temperature fluctuations with time of day, season, or weather are unavoidable using current passive treatment systems. As can be seen in Figure 5, decreasing the temperature throughout the system to 10°C, even while allowing the pH and DO to remain at the field-measured levels, drastically reduces the extent of iron oxidation. Less than 20 mg/l removal is predicted for the entire system at this lower temperature. In contrast, increasing the temperature to 25°C accelerates the removal, at least for those sections following the rip-rap channel.

The ineffectiveness of the upper portion of the system (section AD) is thought to be caused by the poor reaction kinetics resulting from the lower pH and DO in these sections. The effect of increasing the DO, pH and both are seen plotted as lines 3,5, and 6 in Figure 5. If the DO could be increased to 7 mg/l and held there throughout the system (i.e., constant recharge and no depletion due to reaction), the resultant ferrous levels are projected as line 3. The surprisingly small effect is due to the low pH and the square of the hydroxide concentration term in the rate expression. Additional dissolved oxygen is ineffective in the face of this barrier. In contrast, increasing the pH to only 6.5 has a dramatic effect and is plotted as line 5. Not only do the iron levels drop precipitously after the rip-rap channel, but even the more oxygen-starved regions of the channel above the rip-rap section start to become productive. In practice, such a modest pH increase could reasonably be attained by adding a rip-rap channel just after the ALD, or, where constraints at the site prohibit such construction, by actively air sparging the ALD effluent. This practice would increase both the DO and the pH simultaneously. The effect of increasing both the DO to 7 mg/l and the pH to 6.5 is seen as the 6th and bottom-most line in Figure 5. In this scenario, effluent ferrous

Table 3. Comparison of model and literature values. Literature values from Sung and Morgan (1980).

	Regression Estimate	Solver Estimate	Literature
E_{act} (kcal/mole)	68.5	68.5	~ 0
$k_{(25\,oC)}$ (l^2 $mole^{-2}$ atm^{-1} min^{-1})	9.8×10^{14}	8.0×10^{14}	10^{11} - 10^{14}

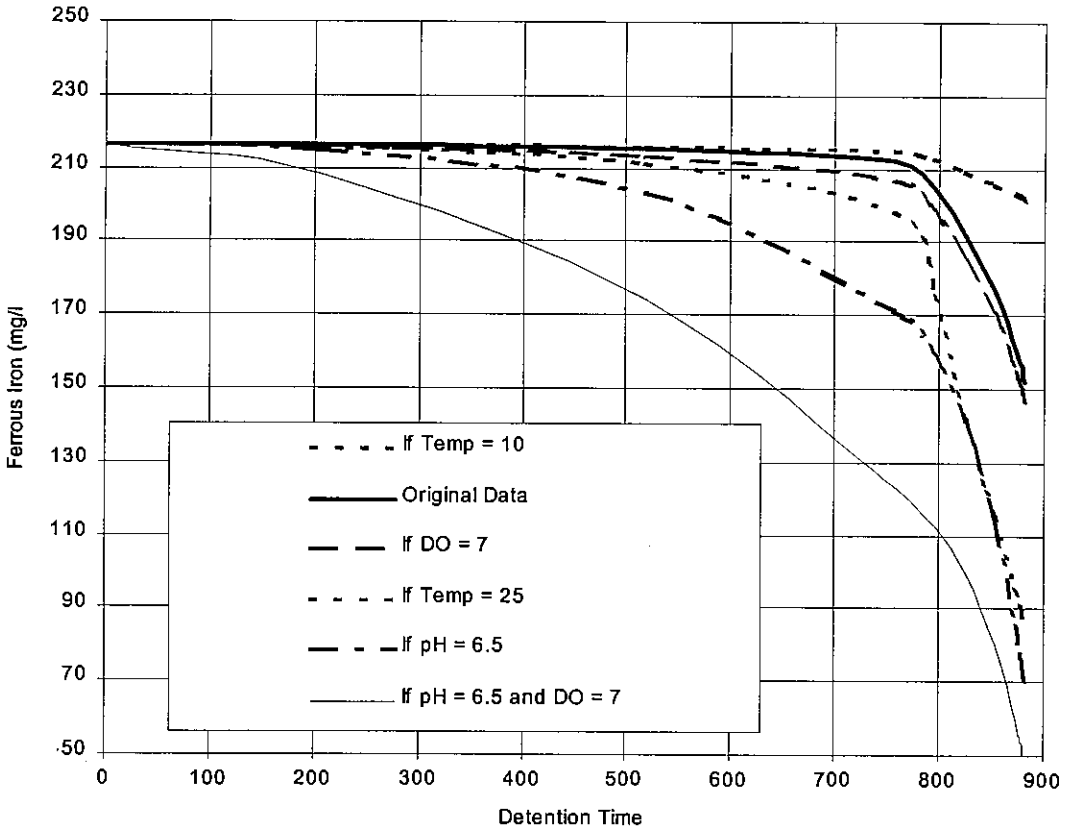

Figure 5. Lines, numbered from top to bottom, represent: (1) as-measured pH and DO, Temperature = 10°C; (2) best fit of model to all of the measured values; (3) as-measured Temperature and pH, DO = 7 mg/l; (4) as-measured pH and DO, Temperature = 25°C; (5) as-measured Temperature and DO, pH=6.5; (6) as-measured Temperature, pH=6.5, DO=7 mg/l.

Table 4. Predicted effluent levels of ferrous iron based on the Solver Estimates.

If **pH** is...	If **D.O.** is...	**Predicted Effluent Concentrations of Fe(II) in mg/L**		
		if **Temperature** is constant at 10°C	if **Temperature** is variable as measured on-site	if **Temperature** is constant at 25°C
variable, as-measured	variable, as-measured	201	152	85
variable, as-measured	constant at 7 mg/L	199	146	73
constant at 6.5	variable, as-measured	168	70	8.6
constant at 6.5	constant at 7 mg/L	147	49	1.5

levels would drop to about 50 mg/l (provided the initial water had sufficient alkalinity). Other scenarios considered but not shown in Figure 5 include maintaining the DO and pH at 7 mg/l and 6.5 as in scenario 6, but also holding the temperature at 25°C. If this could be done, the model predicts effluent levels would meet current environmental standards of less than 3 mg/l. However, such high reaction rates would make it difficult or impossible to maintain the specified pH and oxygen concentrations. Also, maintaining the DO and pH as above but decreasing the temperature to 10°C, reduces the effectiveness to the extent that effluent levels are still in the area of 150 mg/l. The expected effluent ferrous iron concentrations for these various scenarios are presented in Table 4.

Conclusions

The total amount of iron removal at this site is 12.7 $gd^{-1}m^{-2}$ which is within the range reported by Hedin et al. (1994). However, by segmenting the channel and measuring the loss across sections it was seen that the individual removal rates varied from low values below 10 $gd^{-1}m^{-2}$ to some high values over 30 $gd^{-1}m^{-2}$. Higher values always occurred in the well-aerated sections below rip-rap or other turbulent sections, highlighting the importance of placing some type of aeration as close as possible to the alkaline discharge (in this case the ALD effluent).

The ferrous iron levels at the various sampling locations were modeled using a plug-flow approximation of the water-flow in the channel, and literature reaction rate and activation relationships. The model provided a good fit to the data, indicated a large temperature effect, and was used to help understand the behavior of the remediation system. The model supported the importance of aeration and indicated that the pH increase, presumably due to loss of CO_2, was more important than the increase in dissolved oxygen, even in oxygen-poor sections of the channel. The model was further used to predict the effect of additional remediation efforts. It was predicted that increased aeration of the ALD effluent, which would raise both the DO and the pH, could lead to effluent levels as low as 50 mg/L (if sufficiently alkaline) as opposed to the current 150 mg/L. The DO and pH values needed to achieve this efficiency were predicted to be 7 and 6.5 respectively, which can reasonably be attained in field installations. This increased efficiency would correspond to a removal rate of 36 $gd^{-1}m^{-2}$. This value would place the system among the top performers but still within the range found in the study by Hedin et al. 1994.

Literature Cited

American Public Health Association. 1998. Standard Methods for the Examination of Water and Wastewater, 20th ed. APHA, Washington, D.C.

Brodie, G. A. 1991. Achieving compliance with staged aerobic constructed wetlands to treat acid drainage. In: Proceedings of the 1991 National Meeting of the American Society of Surface Mining and Reclamation, ed. by W. Oaks, and J. Bowden. https://doi.org/10.21000/JASMR91010151

Fales, H. A. and F. Kenny. 1940. Inorganic quantitative analysis. D. Appleton Century Co., New York, 713 pp.

Fylstra, D., L. Lasdon and A. Waren. 1998. Design and use of the Microsoft Excel solver. Interfaces 28(5): 29-55. https://doi.org/10.1287/inte.28.5.29

Hedin, R. S., R. W. Nairn and R. L. P. Kleinmann. 1994. Passive treatment of coal mine drainage. U.S. Bureau of Mines IC 9389.

Kirby, C. S., and J. A. Elder Brady. 1998. Field determination of Fe^{2+} oxidation rates in acid mine drainage using a continuously stirred tank reactor. Applied Geochemistry 13: 509-520. https://doi.org/10.1016/S0883-2927(97)00077-2

Kirby, C. S., H. M. Thomas, G. Southman and R. Donald. 1999. Relative contributions of abiotic and biological factors in Fe(II) oxidation in mine drainage. Applied Geochemistry, 14: 511-530. https://doi.org/10.1016/S0883-2927(98)00071-7

Singer and Stumm. 1970. Acidic mine drainage: the rate determining step. Science 167: 1121-1123. https://doi.org/10.1126/science.167.3921.1121

Stark, L., E. Stevens, H. Webster and W. Wenerick. 1990. Iron loading, efficiency and sizing in a constructed wetland receiving mine drainage. In: Proceedings (v.2) of the 1990 Mining and Reclamation Conference and Exhibition, ed. by J. Skousen, J. Sencindiver and D. Samuel. https://doi.org/10.21000/JASMR90020393

Stumm, W. and G. F. Lee. 1961. Oxygenation of ferrous iron. Industrial and Engineering Chemistry, 53: 143-146. https://doi.org/10.1021/ie50614a030

Stumm, W. and J. Morgan. 1981. Aquatic Chemistry. Wiley-Interscience, New York.

Stumm, W. and J. Morgan. 1996. Aquatic Chemistry. Wiley & Sons, New York.

Sung, W. and J. Morgan. 1980. Kinetics and product of ferrous iron oxygenation in aqueous systems. Environ. Sci. Technol. 14: 561-568.
https://doi.org/10.1021/es60165a006

Watzlaf, G. R., K. T. Schroeder, and C. L. Kairies. 2000. Long-term performance of alkalinity-producing passive systems for the treatment of mine drainage. p. 262-274. In: Proceedings of the 1991 National Meeting of the American Society of Surface Mining and Reclamation (Tampa, FL, June 11-1, 2000).

https://doi.org/10.21000/JASMR00010262